Journal of Photochemistry, 4 (1975) 215 - 226

© Elsevier Sequoia S.A., Lausanne — Printed in Switzerland

THE ENERGY POOLING REACTION $2O_2(^1\Delta_g) \rightarrow O_2(^3\Sigma_g^-) + O_2(^1\Sigma_g^+)$; FORMATION, RELAXATION, AND QUENCHING OF VIBRATIONALLY EXCITED $O_2(^1\Sigma_g^+)$

U. SCHURATH

Institut für Physikalische Chemie der Universität Bonn, 53 Bonn, Wegelerstrasse 12 (West Germany)

(Received January 30, 1975)

Summary

Quantitative measurements of the steady state vibrational population of $O_2(^1\Sigma_g^+)_{v=0,1,2}$ from the energy pooling reaction: $2O_2(^1\Delta_g) \rightarrow O_2(^3\Sigma_g^-) + O_2(^1\Sigma_g^+)$, in the presence of strong electronic quenchers of the $^1\Sigma_g^+$ state indicate that this reaction produces $O_2(^1\Sigma_g^+)$ preferentially with two quanta of vibrational excitation. The relative probabilities for the products $O_2(^1\Sigma_g^+)_{v=0}$ and $O_2(^1\Sigma_g^+)_{v=1}$ are lower by roughly a factor of two, and by at least a factor of 17, respectively. The rate constant for vibrational relaxation of $O_2(^1\Sigma_g^+)_{v=2}$ by molecular oxygen, directly to $O_2(^1\Sigma_g^+)_{v=0}$, is found to be $(9 \pm 1) \times 10^{-13}$ cm^3 molecule^{-1} s^{-1}, this value being based on rate constants for electronic quenching of $O_2(^1\Sigma_g^+)$, assumed to be independent of vibrational excitation. This rapid process provides for an extremely efficient vibrational equilibration of $O_2(^1\Sigma_g^+)_v$ in discharged oxygen. The gases NH_3, H_2 and CO_2 are found to act predominantly as electronic quenchers of $O_2(^1\Sigma_g^+)_v$, while CH_4 and C_2H_2 contribute measurably to its vibrational relaxation.

Introduction

Metastable oxygen molecules in the $a^1\Delta_g$ state undergo two types of "reactions" among themselves which are easily detected in flow tubes and static reactors, either by direct light emission, or by light emission from their products. This is due to the long radiative lifetime [1] and low sensitivity of $O_2(^1\Delta_g)$ to quenching collisions [2, 3] which render possible the production of high average concentrations of these molecules in laboratory systems. These "reactions" are the dimole emission (1), which releases the combined excitation energy of two colliding $O_2(^1\Delta_g)$ molecules as radiation, or part of it if one product molecule is formed with vibrational excitation [4, 5], and the energy pooling reaction (2), which produces one $O_2(^1\Sigma_g^+)$ molecule plus one oxygen molecule in the electronic ground state [5, 6]:

$$2O_2(^1\Delta_g)_{v=0} \xrightarrow{a} 2O_2(^3\Sigma_g^-)_{v=0} + h\nu_{6340\ \text{Å}}$$

$$\xrightarrow{b} O_2(^3\Sigma_g^-)_{v=0} + O_2(^3\Sigma_g^-)_{v=1} + h\nu_{7030\ \text{Å}} \quad (1)$$

$$2O_2(^1\Delta_g)_{v=0} \rightarrow O_2(^3\Sigma_g^+)_v + O_2(^1\Sigma_g^+)_v \quad (2)$$

Both reactions have been of practical importance as measures of relative $O_2(^1\Delta_g)$ concentrations in flow tubes [7] and in static systems [2, 8]. The dimole emission has the advantage of being proportional to the square of the $O_2(^1\Delta_g)$ concentration regardless of the total pressure. Reaction (2) proceeds at a rate 10^6 times faster than the dimole emission [5] and produces $O_2(^1\Sigma_g^+)$ molecules which are readily detected by their emission of the atmospheric band, $O_2(^1\Sigma_g^+ \rightarrow {}^3\Sigma_g^-)$ (0,0), at 7619 Å. Although the rate of reaction (2) is proportional to the square of the $O_2(^1\Delta_g)$ concentration as well, the steady state concentration of $O_2(^1\Sigma_g^+)$ is at the same time vefy sensitive to wall collisions and to the presence of quenchers in the gas phase. Several measurements of quenching rate constants for $O_2(^1\Sigma_g^+)$ are based on the pressure dependence of its steady state concentration [2, 9]. A modification of this technique for the detection of vibrationally excited $O_2(^1\Sigma_g^+)$ from the energy pooling reaction (2), and of its vibrational relaxation relative to electronic quenching are presented in this paper.

The energies of reaction (2) are such that up to two vibrational quanta may be distributed, at room temperature, among the products of two $O_2(^1\Delta_g)$ molecules reacting in their vibrational ground state, as summarized in Table 1. Strong emission of $O_2(^1\Sigma_g^+)$ molecules produced by the energy pooling reaction in active oxygen is normally observed from the zeroth vibrational level only, to which most of the published rate constants apply. Derwent and Thrush [5] concluded from flow tube measurements that the energy pooling reaction does populate the first vibrational level as well, with about 5% probability, and measured a rate constant for its quenching and/or relaxation by water molecules which is about 50% higher than that for the lowest vibrational level of $O_2(^1\Sigma_g^+)$. The authors point out that a 20:1 ratio for the production of $O_2(^1\Sigma_g^+)$ in its vibrational levels $v = 0$ and $v = 1$ by the energy pooling reaction is high compared with a 42:1 ratio of the Franck–Condon factors belonging to the corresponding bands of the $(^1\Sigma_g^+ - {}^1\Delta_g)$ transition in isolated oxygen molecules. This paper presents additional evidence that the Franck–Condon concept can by no means be sustained for the vibrational population of $O_2(^1\Sigma_g^+)$ by energy pooling of two $O_2(^1\Delta_g)$ molecules, and that the generally observed near-thermal population of $O_2(^1\Sigma_g^+)$ in active oxygen is merely the result of its rapid vibrational equilibration with $O_2(^3\Sigma_g^-)$.

Experimental

Metastable oxygen molecules $O_2(^1\Delta_g)$ were generated by a microwave discharge in ultrapure oxygen. Oxygen atoms were removed on a HgO film in the discharge region which was continuously regenerated by distilling

TABLE 1

Energetically accessible vibrational excitations in the products of the energy pooling reaction (2)

Vibrational quanta in the products		Energy of reaction, ΔE, (kT = 205 cm^{-1} at 295 K) (cm^{-1})	$\exp(-\Delta E/kT)$
$O_2(^3\Sigma_g^-)$	$O_2(^1\Sigma_g^+)$		
$v = 0$	$v = 0$	−2643.8	
$v = 1$	$v = 0$	−1087.4	
$v = 0$	$v = 1$	−1239.0	
$v = 1$	$v = 1$	+ 317.3	0.21
$v = 2$	$v = 0$	+ 445.4	0.11
$v = 0$	$v = 2$	+ 137.7	0.51

Spectroscopic constants of oxygen were taken from ref. [11].

mercury vapour through the discharge as well. Addition of small amounts of NO_2 to remove traces of oxygen atoms had no effect on the results. The stream of active oxygen was directed through a light trap into a mixing cell where other gases could be admixed. The combined gases were then introduced into a Teflon lined metal tube (7 cm i.d. × 40 cm length) in front of a quartz observation window. The flow tube was mechanically pumped through a flow restrictor. Total pressures in the tube were measured with a MKS Baratron 0 - 10 Torr pressure head (type 235 HS). Before a series of experiments, the system was calibrated by measuring the total pressure in the flow tube as a function of the flow rate, in small increments over the pressure range of interest. From the calibration curve the partial pressures of binary gas mixtures in the flow tube could be calculated from simple pressure measurements, provided that one flow rate, usually that of discharged oxygen, was constant during the experiment.

Emissions in the flow tube were analyzed by a Spex 1704 monochromator which viewed along its axis through the quartz window. A 6100 Å cut-off filter was used for most of the quantitative measurements. The grating (1200 lines/mm) was blazed for 6000 Å. The detection system consisted of a liquid nitrogen cooled EMI 9659 QB photomultiplier tube, a fast pre-amplifier, an Ortec 436 100 MHz discriminator, and an Ortec 449 ratemeter coupled to a strip chart recorder. The relative quantum efficiency of the optical system between 6000 and 8200 Å, calculated from a spectrum of the air afterglow in the flow tube [10], corresponded within experimental accuracy to the quantum efficiency curve of the photomultiplier tube as provided by the manufacturer, falling rapidly below it above 8200 Å.

Results and Discussion

Emission spectra of $O_2(^1\Sigma_g^+)$ from 2 Torr of atom-free active oxygen in

an all-glass flow tube were recorded at 4 Å resolution. The band areas were measured to establish the vibrational population of the emitter generated by the energy pooling reaction (2). The deduced relative photon intensities of the observable vibronic bands, corrected for the relative spectral sensitivity of the detection system, are listed in Table 2, fourth column. Vibrational populations $N_{v'}$, calculated for thermal equilibrium at 295 K, are listed in the second column. These were converted into relative intensities by the formula:

$$I_{v'v''} \sim \sigma^3 q_{v'v''} N_{v'} \qquad \text{(A)}$$

where σ = wavenumber, and are listed in the third column. The Franck–Condon factors $q_{v'v''}$ of the $O_2(^1\Sigma_g^+ - {}^3\Sigma_g^-)$ transition were taken from ref. [11]. Comparison of the measured relative intensities with those calculated for thermal equilibrium, last column of Table 2, indicate that the relative population of the vibrational levels $v' = 0$ and $v' = 1$ is approximately thermal, whereas the $v' = 2$ level is clearly overpopulated. This was the first indication that the second vibrational level of $O_2(^1\Sigma_g^+)$ might be preferentially populated, at least compared with $v' = 1$, by the energy pooling reaction (2). To obtain further information, the primary vibrational population of $O_2(^1\Sigma_g^+)$ from reaction (2) had to be probed more closely, either by measuring emission spectra at extremely low pressures to reduce vibrational relaxation of $O_2(^1\Sigma_g^+)$ within its radiative lifetime, or by adding a strong electronic quencher of $O_2(^1\Sigma_g^+)$ which would be capable of "freezing" the primary vibrational population. Owing to the long radiative lifetime of the emitter [12], extremely low pressures are necessary for the first method to become effective. This has the disadvantage of reducing the $O_2(^1\Delta_g)$ concentration which affects the energy pooling rate quadratically. The resulting loss of intensity is partly compensated for by reduced homogeneous quenching of $O_2(^1\Sigma_g^+)_v$, until wall collisions become the limiting factor. This limitation is governed by the surface to volume ratio. The large spherical reactor of 220 m^3 volume at the Institut fur Physikalische Chemie in Bonn, which has been described in previous publications dealing with both metastable singlet states of the oxygen molecule [2, 8, 13], has an extremely low surface to volume ratio of 0.8 m^{-1}, and was therefore used to measure relative band intensities of the $O_2(^1\Sigma_g^+ - {}^3\Sigma_g^-)$ transition in the mTorr region. The result in Fig. 1 shows a typical low resolution spectrum of 5.8 mTorr of discharged oxygen under steady flow condition. In addition to the intense (0,0) band at 7619 Å, two weak features at 7800 Å and 6970 Å were identified as the (2,2) and (2,1) bands. The corrected intensity ratio of the (2,2) and the (2,1) bands agrees, within experimental accuracy, with the calculated intensity ratio in Table 2, but their intensity relative to the (0,0) band is about a factor of 6000 above thermal equilibrium. The dimole emission is too weak at 5.8 mTorr to be detected by this technique. The (1,0) band at 6884 Å is *not* observed, although the Franck–Condon factor is only 50% lower than for the (2,1) band. It is concluded that, under the experimental conditions, the

TABLE 2

Relative band intensities of the $O_2(^1\Sigma_g^+ \rightarrow {}^3\Sigma_g^-)$ transition in active oxygen, compared with a calculated vibrational population of $O_2(^1\Sigma_g^+)$ for thermal equilibrium at 295 K

Vibronic band ($v'v''$)	Calculated relative vibrational population for thermal equilibrium at 295 K	Calculated relative band intensities for thermal equilibrium at 295 K	Measured relative band intensities in active oxygen	Ratio of measured to calculated intensities
(0,0)	1	1	1*	1*
(0,1)		4.9×10^{-2}	8.8×10^{-2}	1.8
(1,0)	1.06×10^{-3}	1.0×10^{-4}	2.8×10^{-4}	2.8
(1,1)		8.7×10^{-4}	2.2×10^{-3}	2.5
(2,1)	1.3×10^{-6}	1.4×10^{-7}	**	
		8.4×10^{-7}	5.8×10^{-5}	69

*A metal sieve was used to attenuate the intense (0,0) band. The attenuation factor of the sieve was not well defined, making this measurement imprecise. Comparison of other band intensities should be made relative to the (0,1) band.

**This band was positively identified, but the intensity could not be measured with reasonable accuracy due to the underlying dimole emission.

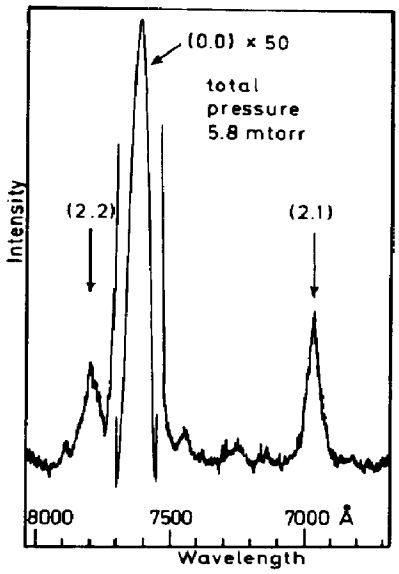

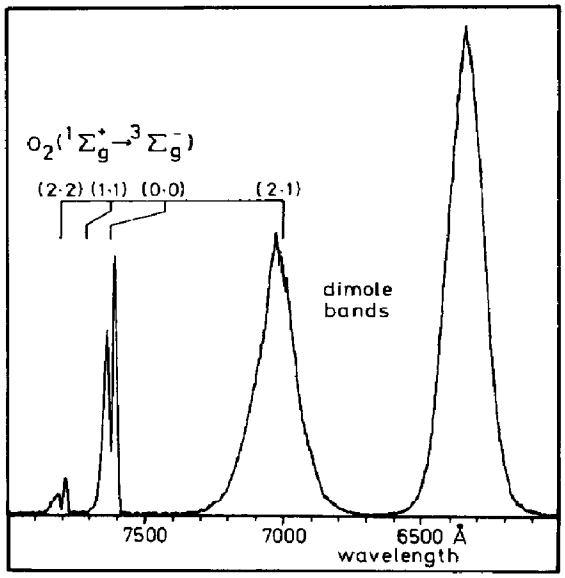

Fig. 1. Low resolution spectrum of 5.8 mTorr active oxygen in a 220 m^3 reactor; three bands of the $O_2(^1\Sigma_g^+ \rightarrow {}^3\Sigma_g^-)$ transition are observed.

Fig. 2. Emission spectrum of 1.9 Torr active oxygen in the presence of 0.6 Torr ammonia.

concentration of $O_2(^1\Sigma_g^+)_{v=2}$ already exceeds that of $O_2(^1\Sigma_g^+)_{v=1}$. Strictly speaking, the observed vibrational distribution was not that of a low pressure spectrum by the definition given above, but rather a partly "frozen" distribution produced by collisions of $O_2(^1\Sigma_g^+)_v$ with the reactor wall which acts as a strong electronic quencher.

Better results were obtained by the second method, the "freezing" of the vibrational population of $O_2(^1\Sigma_g^+)_v$ from reaction (2) by homogeneous quenching. The flow system and the technique of these measurements have been outlined in the experimental section. Strong electronic quenchers of $O_2(^1\Sigma_g^+)$ are ideally suited for this purpose provided that they are also weak quenchers of the precursor molecule $O_2(^1\Delta_g)$. Inspection of quenching rate data [2, 3] shows that the hydrides H_2, NH_2, H_2O, C_2H_2, CH_4, and also the non-hydride CO_2 meet these requirements. The flow rate of the quencher was changed in small increments at constant oxygen flow through the discharge, and the dimole emission as well as the (0,0), (1,1), and the (2,2) bands of the $O_2(^1\Sigma_g^+ \rightarrow {}^3\Sigma_g^-)$ transition were scanned for each mixing ratio at 24 Å resolution. Figure 2 gives an example of a spectrum obtained in the presence of ammonia. A resolution of 8 Å was chosen to emphasize the characteristic contours of the atmospheric bands. One set of data from a series of spectra in the presence of NH_3 is summarized in Fig. 3, where the intensities on a logarithmic scale are shown as a function of $p_{NH_3}; p_{O_2}$ which changed with total pressure at a fixed oxygen flow rate is also given. The intensity ratios may be converted into relative vibrational populations by means of eqn. (A). Values of $\sigma^3 q_{v'v''}$ for the (0,0), (1,1), and (2,2) bands from ref. [11] are 2.103×10^{12}, 1.729×10^{12}, and 1.373×10^{12}, respectively. Addition of NH_3 changes the vibrational population of $O_2(^1\Sigma_g^+)$ in active oxygen from near thermal to completely non-thermal. The intensity of the (1,1) band drops below the (2,2) band, even at the lowest ammonia pressure of 0.02 Torr in 2.5 Torr oxygen, and the (0,0) band approaches the (2,2) band intensity, which changes comparatively little with ammonia pressure. The intensity of the dimole emission (in arbitrary units) is included as a measure of the reaction rate (2). Essentially similar dependences were obtained with H_2, CO_2, C_2H_2, and CH_4, and the effect was qualitatively confirmed with H_2O.

A simple kinetic scheme for the generation, relaxation and quenching of $O_2(^1\Sigma_g^+)_v$ in discharged oxygen will now be used to analyze the experimental data. From the limited information about the elementary steps involved, some simplifying assumptions will be made and discussed. One basic assumption is that *electronic* quenching of $O_2(^1\Sigma_g^+)_v$ is not strongly dependent on vibrational excitation of the metastable molecule. Electronic quenching of $O_2(^1\Sigma_g^+)$ is believed to populate the $^1\Delta_g$ state of oxygen predominantly [3, 9], the released energy being converted into vibrational excitation of the quencher. This has recently been shown in detail by Ogryzlo and Thrush [14], who observed infra-red emission from vibrationally excited CO_2 and water vapour when these were added to active oxygen. The probability for this energy transfer process should be approximately equal for low lying vibrational levels of $O_2(^1\Sigma_g^+)$ since the wavenumbers of the (0,0), (1,1), and (2,2) bands of the $(^1\Sigma_g^+ - {}^1\Delta_g)$ transition, 5239 cm^{-1}, 5160 cm^{-1}, and 5079 cm^{-1}, are close together. If anything, a slight *increase* of the quenching rate constant for higher vibrational levels might be anticipated.

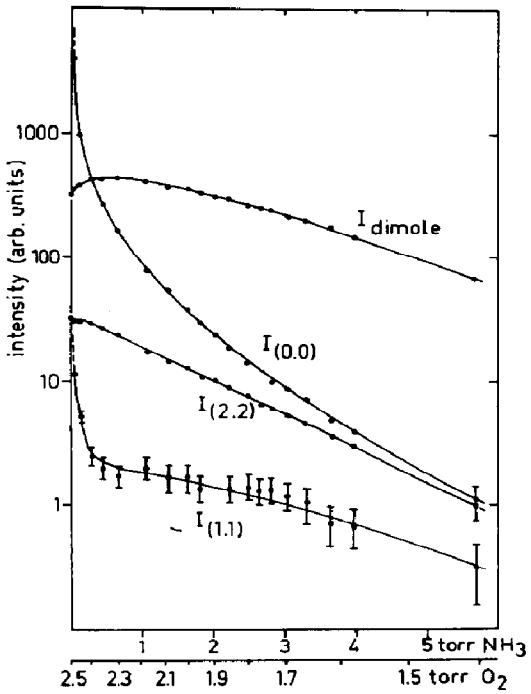

Fig. 3. Relative band intensities of the $O_2(^1\Sigma_g^+ \rightarrow {}^3\Sigma_g^-)$ transition in active oxygen as a function of (NH_3), corrected for spectral response of the detection system. The intensity of the dimole emission at 6340 Å, in arbitrary units, is included as a measure of the energy pooling rate.

Our experimental results indicate that the second vibrational level of $O_2(^1\Sigma_g^+)$ is preferentially populated by the energy pooling process (2). The observed weak dependence of the (2,2) band on the partial pressure of strong electronic quenchers (*cf.* Fig. 3) is easily explained if molecular oxygen in the electronic ground state causes vibrational relaxation of $O_2(^1\Sigma_g^+)_{v=2}$ at a rate comparable to electronic quenching by the added gases. A substantially lower quenching rate constant for this vibrational level would be a most improbable assumption. Generation and removal of $O_2(^1\Sigma_g^+)_{v=2}$ in the flow tube may then be accounted for by the following set of reactions:

$$\Delta + \Delta \xrightarrow{k_2} (2) + O_2 \quad \text{(rate proportional to } I_{\text{dimole}}) \tag{2}$$

$$(2) + O_2 \xrightarrow{k_{tr}} (1) \text{ or } (0), + O_2 \quad \text{(relaxation to } v = 1 \text{ or } 0) \tag{3}$$

$$(2) + M \xrightarrow{k_{rm}} (1) + M \quad \text{(relaxation)} \tag{4}$$

$$(2) + M \xrightarrow{k_q} O_2 + M \text{ (electronic quenching)} \tag{5}$$

Δ denotes the $O_2(^1\Delta_g)$ state, and (0), (1) and (2) means $O_2(^1\Sigma_g^+)$ in its zeroth, first and second vibrational levels. Wall removal as well as electronic quenching of $O_2(^1\Sigma_g^+)$ by $O_2(k_q(O_2) = 4.7 \times 10^{-17}$ cm^3 molecule^{-1} s^{-1} [15]) may be neglected as soon as the partial pressure of even the weakest

quencher used in these experiments, CH_4, exceeds 50 mTorr in 2.5 Torr oxygen. The steady state concentration of $O_2(^1\Sigma_g^+)_{v=2}$ in the presence of a quencher M may then be written as follows:

$$(2) = \frac{(\Delta)^2 \times k_2}{k_{tr}(O_2) + k_{tm}(M)} \qquad \text{(B)}$$

$k_{tm} = k_q + k_{rm}$ summarizes the rate constants for electronic quenching as well as vibrational relaxation by the additive M. Rearrangement of eqn.(B) yields an expression for the intensity ratio of the dimole emission, I_d, and the (2,2) band at 7804 Å, I_2, as a function of the pressure ratio $(M)/(O_2)$:

$$\text{const.} \times \frac{I_d}{I_2} \times \frac{1}{(O_2)} = k_{tr} + k_{tm}(M)/(O_2) \qquad \text{(C)}$$

Plots of $I_d/I_2(O_2)$ *versus* $(M)/(O_2)$ should be linear, with constant intercepts on the ordinate. The ratio intercept/slope, multiplied by $k_q = k_{tm} - k_{rm}$, is a lower limit of the rate constant k_r for vibrational relaxation of $O_2(^1\Sigma_g^+)_{v=2}$ by oxygen. Three independent sets of data, measured with NH_3 as quencher M in the presence of 1.1 to 4.1 Torr oxygen, are plotted according to eqn. (B) in Fig. 4. Linear plots, with different slopes were also obtained for M = CO_2, H_2, C_2H_2, and CH_4. The intercepts on the ordinate were identical to that in Fig. 3 within experimental accuracy. The measured intercept/slope ratios are summarized in the third column of Table 3. Combining these with literature values of k_q, assumed to be independent of v', a lower limit of $(9 \pm 1) \times 10^{-13}$ cm^3 molecule^{-1} s^{-1} is obtained in column four for vibrational relaxation of $O_2(^1\Sigma_g^+)_{v=2}$ by oxygen. If, by analogy with $O_2(^1\Delta_g)_{v=1}$ which has been investigated by Collins and Husain [19], the rate constant k_{rm} for vibrational relaxation by simple diatomic quenchers is small compared with $4 \times 10^{-14} = k_q(H_2)$ [2, 16], then the value of $(9 \pm 1) \times 10^{-13}$ cm^3 molecule^{-1} s^{-1} may actually be equated with k_r. This corresponds to an efficiency of 1 in 250 hard sphere collisions for vibrational relaxation of $O_2(^1\Sigma_g^+)_{v=2}$ by oxygen.

Although the comparatively low values for CH_4 and C_2H_2 in column 4 of Table 3 may be insignificant in view of the limited accuracy of the rate constants k_q summarized in column 2, they probably indicate an increasingly important contribution of vibrational relaxation by C_2H_2 and CH_4 to the removal of $O_2(^1\Sigma_g^+)_{v=2}$. This expectation is supported by the recent data of Collins and Husain [19] who report rate constants of 6.7×10^{-14} and 1.1×10^{-13} cm^3 molecule^{-1} s^{-1} for vibrational relaxation of $O_2(^3\Sigma_g^-)_{v=1}$ and $O_2(^1\Delta_g)_{v=1}$ by CF_4. Our finding that CH_4 is very efficient is also confirmed by literature data on the relaxation of vibrationally excited oxygen in its electronic ground state [20].

The high rate constant k_{tr} for vibrational relaxation of $O_2(^1\Sigma_g^+)_{v=2}$ by oxygen may be accounted for either by a stepwise transfer of single vibrational quanta from the metastable molecule into the vibrational ladder of ground state oxygen, and/or by a rapid exchange of electronic excitation with $O_2(^3\Sigma_g^-)_{v=0}$. Such an exchange process was established by

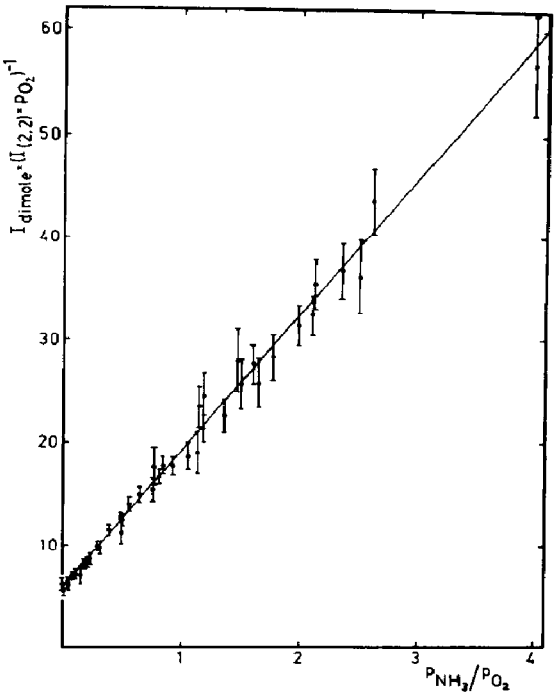

Fig. 4. $I_d/I_2(O_2)$ plotted as a function of $[NH_3]/[O_2]$, according to eqn. (C).

TABLE 3

Ratios of intercept/slope according to eqn. (C) for H_2, NH_3, CO_2, C_2H_4, and CH_4

Gas, M	$k_q \times 10^{13}$ (cm^3 $molecule^{-1}$ s^{-1})		Intercept/ slope	$k_q \times$ intercept/slope $\times 10^{13}$ (cm^3 $molecule^{-1}$ s^{-1})
H_2	4.0	[2, 16]	2.4	9.5
NH_3	18	[2]	0.45	8.0
CO_2	3.3	[17, 3]	2.8	9.2
C_2H_2	2.5 (4.5)	[2, 18]	1.7	4.3 (7.7)
CH_4	0.75		1.3	1.0

Jones and Bayes [21] to occur between $O_2(^1\Delta_g)_{v=0}$ and $O_2(^3\Sigma_g^-)_{v=0}$ in at least 1 out of 10 hard sphere collisions. Its analogue is indistinguishable in our system from vibrational relaxation of $O_2(^1\Sigma_g^+)_{v=2}$ directly to $v = 0$. However, vibrational relaxation by oxygen in steps of either one or two vibrational quanta at a time must have a bearing upon the steady state concentration of $O_2(^1\Sigma_g^+)_{v=1}$ in the presence of electronic quenchers and may thus be distinguished. The following reaction scheme provides for both modes of vibrational relaxation:

$$\Delta + \Delta \xrightarrow{k_{0,1,2}} (0) \text{ or } (1) \text{ or } (2) \tag{2}$$

$$(2) + O_2 \xrightarrow{k_r^{2,0}} (0) + O_2 \quad \text{(relaxation in steps of } \Delta v = 2\text{, or exchange of electronic excitation)} \tag{3a}$$

$$(2) + O_2 \xrightarrow{k_r^{2.1}} (1) + O_2$$ (exchange of electronic excitation unimportant because of low concentration of $O_2(^3\Sigma_g^-)_{v=1}$) (3b)

$$(1) + O_2 \xrightarrow{k_r^{1.0}} (0) + O_2$$ ("normal" relaxation, or exchange of vibrational excitation) (3c)

$$(2), (1) + M \xrightarrow{k_{rm}} (1), (0) + M \quad (4)$$

$$(2), (1), (0) + M \xrightarrow{k_q} O_2 + M \quad (5)$$

(The rate constants k_{rm} and k_q are assumed to be independent of v'.) A steady state treatment yields the following concentration ratio for $O_2(^1\Sigma_g^+)$ in its first and second vibrational levels:

$$\frac{(1)}{(2)} = \frac{k_1}{k_2} \times \frac{(k_r^{2.0} + k_r^{2.1})(O_2) + k_{tm}(M)}{k_r^{1.0}(O_2) + k_{tm}(M)} + \frac{k_r^{2.1}(O_2) + k_{rm}(M)}{k_r^{1.0}(O_2) + k_{tm}(M)} \quad (D)$$

With the reasonable assumption that $k_r^{2.0} + k_r^{2.1} = k_{tr} \geqslant k_r^{1.0}$, this equation may be approximated by:

$$\frac{(1)}{(2)} \geqslant \frac{k_1}{k_2} + \frac{k_r^{2.1}(O_2) + k_{rm}(M)}{k_r^{1.0}(O_2) + k_{tm}(M)} \quad (D')$$

According to our data in Fig. 4, combined with the appropriate values of $\sigma^3 q_{v'v''}$ [11], the ratio (1):(2) is as low as 0.06 for 0.5 Torr NH_3 and 2.35 Torr O_2. This is in fact an upper limit for the rate constant ratio k_1/k_2 pertaining to the formation of $O_2(^1\Sigma_g^+)$ in $v' = 1$ and $v' = 2$ by the energy pooling reaction (2). At the specified pressures, the second term in eqn. (D′) cannot exceed the value of 0.06 either. An estimate of the second term in (D′) can be obtained from the ratio $k_{tr}/k_{tm} = (k_r^{2.0} + k_r^{2.1})/k_{tm} =$ 0.45 for NH_3 in Table 3. A value greatly in excess of 0.06 would result if k_{tr} were approximately equal to $k_r^{2.1}$, as one would expect for "normal" vibrational relaxation by oxygen in steps of $\Delta v = 1$. It is therefore concluded that $k_r^{2.1}$ is much smaller than $k_r^{2.0}$.

Higher ratios of (1):(2) were observed for CH_4 and, to a lesser extent, for C_2H_2 as quenchers, approaching a value close to unity at high CH_4 concentrations. This supports the conclusion that vibrational relaxation of $O_2(^1\Sigma_g^+)_v$ by CH_4 and C_2H_2 is fast compared with electronic quenching by these gases.

Rearrangement of the steady state equation for $O_2(^1\Sigma_g^+)_{v=0}$, based on the set of reactions (2) - (5), yields the following expression for the concentration ratio of the zeroth and second vibrational levels:

$$\frac{(0)}{(2)} = \frac{[O_2]}{[M]}\left(\frac{k_0 k_{tr}}{k_2 k_q} + \frac{(1)k_r^{1.0}}{(2)k_q} + \frac{k_r^{2.0}}{k_q}\right) + \left(\frac{k_0 k_{tm}}{k_2 k_q} + \frac{(1)k_{rm}}{(2)k_q}\right) \quad (E)$$

In the presence of the strong electronic quenchers NH_3, H_2 and CO_2, the ratio (1):(2) was observed to be much smaller than unity and only weakly pressure dependent (*cf.* Fig. 4). A plot of the intensity ratio I_0/I_2 *versus*

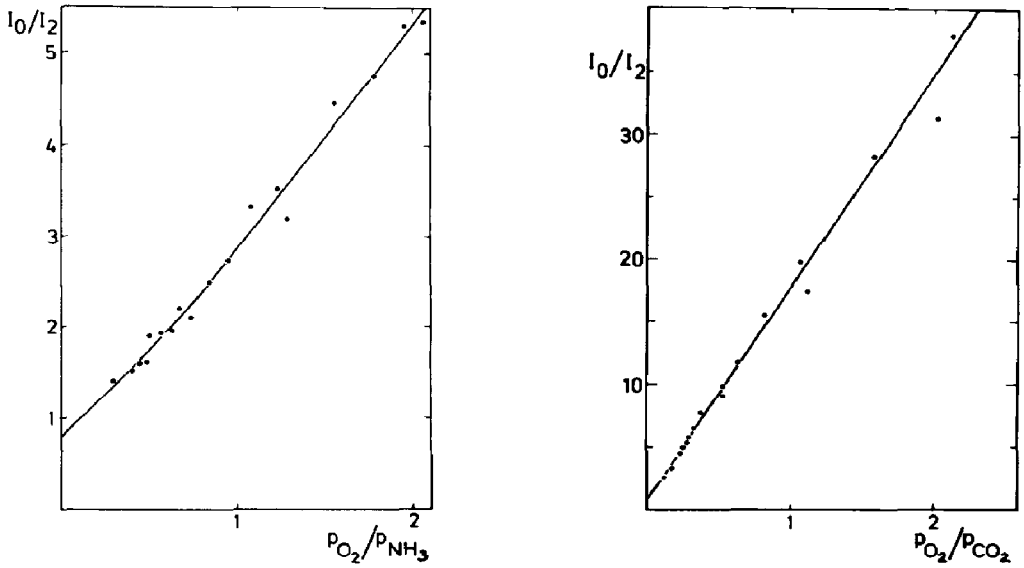

Fig. 5. I_0/I_2 plotted as a function of $[O_2]/[M]$ for M = NH_3 and H_2, and extrapolated to $[O_2]/[M] = 0$ according to eqn. (E).

$[O_2]/[M]$ should therefore yield approximately straight lines for these gases, with a non-zero intercept. Our results for NH_3 and CO_2 are plotted accordingly in Fig. 5. They confirm this expectation, as do the data for H_2 which are not shown in the Figure, yielding the same intercepts within experimental accuracy. These are 0.8 ± 0.3, 0.8 ± 0.5 and 0.9 ± 0.5, respectively. The intensity ratios I_0/I_2 for C_2H_2 also fitted on a reasonably straight line which extrapolated, however, to an intercept of 3 ± 2. A plot of I_0/I_2 *versus* $[O_2]/[M]$ showed considerable curvature and could not be extrapolated with reasonable accuracy.

The extrapolated intensity ratio $(I_0/I_2)_{lim} = 0.8 \pm 0.3$ for strong electronic quenchers corresponds to a concentration ratio $[(0)/(2)]_{lim}$ of 0.5 ± 0.2. Comparison of this value with the second term of eqn. (E) in square brackets shows that this is an upper limit for the rate constant ratio k_0/k_2. Values of $[(0)/(2)]_{lim}$ in excess of 0.5 are expected for gases which contribute appreciably to vibrational relaxation of the metastable state, in agreement with our findings for C_2H_2.

In summary it can be said that the predominant primary product of the energy pooling reaction (2) is vibrationally excited $O_2(^1\Sigma_g^+)_{v=2}$. $O_2(^1\Sigma_g^+)_{v=0}$ is produced at roughly half its rate, whereas the probability for the formation of $O_2(^1\Sigma_g^+)_{v=1}$ is at least a factor of 17 lower. These probabilities do not correlate with the Franck–Condon factors of the corresponding optical transitions $O_2(^1\Sigma_g^+ - {}^1\Delta_g)$ (v',v'') which are $q_{0.0} = 0.976$, $q_{1.0} = 2.3 \times 10^{-2}$, and $q_{2.0} = 3.7 \times 10^{-4}$ [22]. It appears that reaction (2) is fastest if one of the products, either $O_2(^1\Sigma_g^+)$ or $O_2(^3\Sigma_g^-)$, is produced with two quanta of vibrational excitation, while all other combinations listed in Table 1 are less favourable. If this concept is correct, the observed rate constant ratio $k_0/k_2 = 0.5 \pm 0.2$ for the products $O_2(^1\Sigma_g^+)_{v=0}$ and $O_2(^1\Sigma_g^+)_{v=2}$

may to some extent be attributed to a difference in activation energies as indicated in the last column of Table 1.

Although vibrational equilibration of $O_2(^1\Sigma_g^+)_v$ from the energy pooling reaction (2) by oxygen is extremely rapid, competitive quenching of $O_2(^1\Sigma_g^+)_{v=2}$ from the primary process may become important at higher concentrations of strong electronic quenchers. This has to be considered if quenching rate constants or other kinetic data are to be derived from intensity measurements of the $O_2(^1\Sigma_g^+ \rightarrow {}^3\Sigma_g^-)$ (v', v'') transition in active oxygen. Similar complications may arise in flash photolysis systems where $O_2(^1\Sigma_g^+)$ is generated by the reaction of $O(^1D)$ atoms with ground state molecular oxygen [18]. This process, being near resonant for $v' = 2$, may produce vibrationally excited $O_2(^1\Sigma_g^+)$ as well.

Acknowledgement

Support of this work by the Deutsche Forschungsgemeinschaft is gratefully acknowledged.

References

1 R. M. Badger, A. C. Wright and R. F. Whitlock, J. Chem. Phys., 43 (1965) 4345.
2 K. H. Becker, W. Groth and U. Schurath, Chem. Phys. Lett., 8 (1971) 259; R. D. Penzhorn, H. Güsten, U. Schurath and K. H. Becker, Env. Sci. Technol., 8 (1974) 907.
3 J. A. Davidson and E. A. Ogryzlo, in Chemiluminescence and Bioluminescence, Plenum Press, New York, 1973, p. 111.
4 L. W. Bader and E. A. Ogryzlo, Discuss. Faraday Soc., 37 (1964) 46.
5 R. G. Derwent and B. A. Thrush, Trans. Faraday Soc., 67 (1971) 2036.
6 S. J. Arnold and E. A. Ogryzlo, Can. J. Phys., 45 (1967) 2053.
7 E. A. Ogryzlo and C. W. Tang, J. Am. Chem. Soc., 92 (1970) 5034; K. Furukawa and E. A. Ogryzlo, Chem. Phys. Lett., 12 (1971) 370; K. Furukawa and E. A. Ogryzlo, J. Photochem., 1 (1972/73) 163.
8 K. H. Becker, W. Groth and U. Schurath, Chem. Phys. Lett., 14 (1972) 489.
9 J. A. Davidson and E. A. Ogryzlo, Can. J. Chem., 52 (1974) 240.
10 A. Fontijn, C. B. Meyer and H. I. Schiff, J. Chem. Phys., 40 (1964) 64.
11 P. H. Krupenie, J. Phys. Chem. Ref. Data, 1 (1972) 423.
12 J. H. Miller, R. W. Boese and L. P. Giver, J. Quant. Spectrosc. Radiat. Transfer, 9 (1969) 1507.
13 W. Groth *et al.*, Naturwissenschaften, 59 (1972) 379.
14 E. A. Ogryzlo and B. A. Thrush, Chem. Phys. Lett., 24 (1974) 314.
15 R. G. O. Thomas and B. A. Thrush, in print.
16 R. J. O'Brien Jr. and G. H. Myers, J. Chem. Phys., 5 (1972) 3832.
17 R. Scholz, Diplomarbeit, Universität Bonn (1974).
18 F. Stuhl and H. Niki, Chem. Phys. Lett., 5 (1970) 673.
19 R. J. Collins and D. Husain, J. Photochem., 1 (1973) 481.
20 G. M. Burnett and A. M. North (eds.), Transfer and Storage of Energy by Molecules, Wiley, London, 1969, pp. 242, 247.
21 I. T. N. Jones and K. D. Bayes, J. Chem. Phys., 57 (1972) 1003.
22 R. W. Nicholls, J. Res. Nat. Bur. Stand., A69 (1965) 369.